sciendo Powder Metallurgy Progress, Vol.19 (2019), No.1, p.034-043
http://dx.doi.org/10.1515/pmp-2019-0004

POLYMORPHS OF NEODYMIUM NIOBATE AND TANTALATE THIN FILMS PREPARED BY SOL-GEL METHOD

H. Brunckova, Ľ. Medvecký, E. Múdra, A. Kovalčiková

Abstract

Neodymium niobate NdNbO4 (NNO) and tantalate NdTaO4 (NTO) thin films (~100 nm) were prepared by sol-gel/spin-coating process on Pb(Zr0.52Ti0.48)O3/Al2O3 substrates with annealing at 1000°C. The precursors of films were synthesized using Nb or Ta tartrate complexes. The XRD results of NNO and NTO films confirmed tetragonal T-NdNbO4 and T-NdTaO4 phases, respectively, with traces of monoclinic M-NdNbO4 and M´-NdTaO4. The surface morphology and topography were investigated by SEM and AFM analysis. NTO was smoother with roughness 5.24 nm in comparison with NNO (6.95 nm). In the microstructure of NNO, small spherical (~ 20-50 nm) T-NdNbO4 and larger needle-like particles (~100 nm) of M-NdNbO4 phase were observed. The compact clusters composed of fine spherical T-NdTaO4 particles (~ 50 nm) and cuboidal M´-NdTaO4 particles (~ 100 nm) were found in NTO. The results of this work can contribute to formation of different polymorphs of films for the application in environmental electrolytic thin film devices.

Keywords: sol-gel, thin films, NdNbO4, NdTaO4, polymorphs, microstructure

INTRODUCTION

Neodymium orthoniobate NdNbO4 (NNO) and orthotantalate NdTaO4 (NTO) thin films with fergusonite structure have attracted a great deal of attention due to their interesting physical properties, such as high dielectric constants, electro-optical, photoelastic, photocatalytic and luminescent properties as well as good mechanical and chemical stability [1,2]. For lanthanide Ln (Ln = Nd, Sm, Eu and Gd) orthoniobates, there are two crystalline forms, the low temperature M-phase isostructural with monoclinic form of the fergusonite and the T-phase corresponding to tetragonal scheelite. The transition between the two phases occurs reversibly in the range 500-800°C [3]. The NdTaO4 crystallize in monoclinic form, besides their ability to posses two-fergusonite-type structures, first known as M-type (I2/a) and second called M´-type (P2/a). NdTaO4 exist in three polymorphs (T, M and M´) [4-7].

Helena Brunckova, Ľubomír Medvecký, Erika Múdra, Alexandra Kovalčiková: Institute of Materials Research of Slovak Academy of Sciences, Watsonova 47, 040 01 Košice, Slovak Republic

NNO and NTO precursors of thin films can be prepared by different methods: conventional solid state reaction (SSR) [8,9], hydrothermal [10] and sol-gel [1,2]. The sol-gel method has been used to prepare NdNbO4 and NdTaO4 at low temperature [1]. The NNO precursor powders were prepared using the sol-gel method and obtained at 900°C single NdNbO4 phase [2]. The nanocrystalline NNO powders were prepared by sol-gel process and annealing at 1000°C [11]. High quality NTO films on silica glass substrate were prepared by modified sol-gel process and heating at 1200°C with a single monoclinic M′ phase and NTO film composed of M′-type and tetragonal T-type NdTaO4 [12].

Recently, several groups published studies on the relationship between electrical behavior and phase and crystallographic orientation by the introduction of buffer layers such as SrRuO3, LaNiO3, SrTiO3, (La,Sr)MnO3, (La,Sr)CoO3 as an effective method to improve properties of thin films [13,14]. The significant impact of SrTiO3 [13] or (La,Sr)CoO3 [14] acting as buffer layers on structural, microstructural and ferroelectric properties for (Bi,Nd)4Ti3O12 or (Pb,Ca)TiO3 thin films was clearly revealed. By using PbTiO3 and (Pb0.72La0.28)TiO3 or Pb(Zr0.52Ti0.48)O3 (PZT) interlayer it was possible to control the PZT film orientation [15,16].

In this work, we demonstrate a method to prepare novel NdNbO4 and NdTaO4 thin films from polymeric Nb and Ta-tartrate solutions by sol-gel/spin-coating process. We also report the structural properties and morphology of NNO and NTO thin films deposited on the alumina substrates with PZT interlayer and annealed at 1000°C. The results of this work can contribute to the fabrication of these films for application in environmental electrolytic thin film devices.

EXPERIMENTAL

NdNbO4 (NNO) and NdTaO4 (NTO) precursors were prepared by modified polymeric complex sol-gel method [17]. The novel NNO or NTO sol precursors were synthesized from Nd(NO3)3 and Nb- or Ta-tartrate complex in solvent (ethylene glycol, (EG)) with molar ratio of Nd/Nb or Nd/Ta = 1/1. The mole ratio of tartaric acid (TA):EG = 3:1. After homogenization at 80°C, the solutions were stirred, heated at 130°C for 5 hours with the formation of transparent viscous sols. Basic (0.5 M) sols were diluted in stabilization solution (n-propanol). The sols remained stable at room temperature for two months. Pb(Zr0.52Ti0.48)O3 (PZT) sol was prepared by sol-gel method [18]. The raw materials, lead acetate trihydrate and zirconium acetylacetonate were dissolved separately at a temperature of 80°C in glacial acetic acid in two closed flasks. The solutions were dehydrated at 105°C for 2 hours and, after cooling to 80°C, they were mixed with titanium orthotetrabutylate Ti(OR)4 in the required ratio of Pb:Zr:Ti = 1:0.52:0.48. After adding ethylene glycol at the temperature 80°C, an orange sol was formed. The PZT sol concentration after dilution with n-propanol was 1.0 M.

NdNbO4 and NdTaO4 thin films were prepared from the sols synthesized in the stoichiometric ratio and deposited on Al2O3 substrates. The alumina substrates were spin-coated with PZT sol precursor at 2000 rpm for 30 s (PZT interlayer). Single NNO or NTO film layer was deposited on PZT/Al2O3 substrate with a drying step at 110°C for 3 min and calcined at 400°C for 3 min. The coating cycling was repeated three times to obtain three layers of thin films. The final 3-layered NNO and NTO films were annealed at 1000°C for 1 hour in air.

The thermal decomposition of gels were analysed by differential scanning calorimetry, thermogravimetric analysis (JUPITER STA 449-F1 NETZSCH). The phase composition of films was determined by X-ray diffraction analysis (XRD), (a model X' Pert Pro, Philips, The Netherlands) using CuKα radiation. The Raman spectra were

collected by Raman spectroscopy (HORIBA BX 41TF). The surface of film microstructures were characterized using SEM equipped with a focused ion beam (FIB-SEM), (Auriga Compact, Carl Zeiss Germany). Surface topography and root mean square roughness of films were characterized by atomic force microscopy (AFM, Aicon).

RESULTS AND DISCUSSION

The TG and DSC curves of prepared xerogels heated to 1300°C in air are shown in Fig.1. The small weight losses of 6% at temperatures up to 200°C are due to the evaporation of remains of water residuals and ethylene glycol. It was shown that all chemical reactions involving weight loss, such as decomposition of organic polymeric network, finished below 500°C. In Figure 1, the exothermic peaks at 323 and 344°C (NNO) could be attributed to thermal decomposition of tartrate complexes with a corresponding approx. 47.3% (NNO) weight loss. The formation of amorphous oxides started above 400°C with small exo-effects. The presence of small exothermic peaks between 450 and 600°C is the result of the combustion of residual carbon and following crystallization of NdNbO4 phase at 640°C (fluorite tetragonal phase unknown structure denoted as T′ when it is prepared from amorphous) [1]. The exothermic effect above 890°C (NNO) corresponds to the transformation from T′ to the stable T or M phase. In the DSC curve of NNO, the broad and distinct endothermic peak above 1090°C characterizes the T-M transformation of NdNbO4. The last approximately 6% weight loss on TG curve between 900 to 1300°C relates to the above transformations. On the basis of TG analysis, the total weight losses were about 53% (NNO). DSC analysis showed the broad exothermic peaks at 328 and 625°C (NTO) which correspond to organic removal by oxidation with weight losses of about 40.0% (NTO). The two small exothermic peaks at 900 and 994°C (NTO) were observed. The first exo-peak is caused by crystallization of T′ phase and the second correspond to the residual carbon oxidation. The next exothermic peak at 1070°C (NTO) related to transformation from metastable fluorite T′ structure to T or M′ phase. The distinct endothermic peak above 1200°C characterizes the T-M transformation of NdTaO4. The three stage of weight losses above 1200°C are visible on TG curves of NTO xerogel over the temperature range 200°C, 700°C and 1200°C. From TG analysis is resulted that the total weight losses were 51% (NTO).

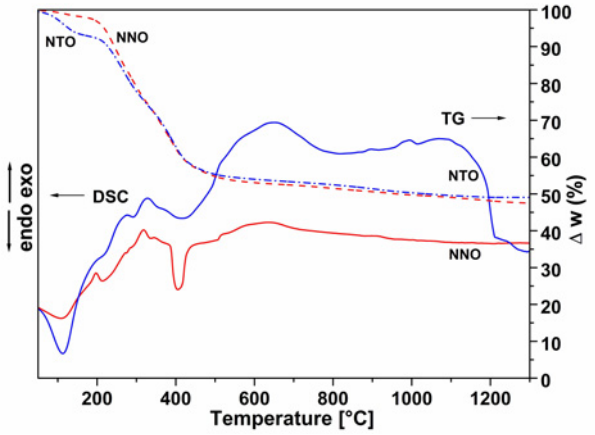

Fig.1. DSC and TG curves of $NdNbO_4$ (NNO) and $NdTaO_4$ (NTO) gel precursors.

The XRD diffractograms of NNO and NTO thin films deposited on PZT/Al_2O_3 substrates and annealed at 1000°C are shown in Fig.2. The XRD analyses verified formation of the monoclinic ZrO_2 (JCPDS 83-0944) in PZT, tetragonal T-$NdNbO_4$ (81-1974) and monoclinic M-$NdNbO_4$ (32-0680) in NNO, tetragonal T-$NdTaO_4$ (16-0745) and monoclinic M´-$NdTaO_4$ (83-0408) phases in NTO. From XRD patterns it resulted that the major phase is T-$NdNbO_4$ in NNO. Lanthanide tantalates usually crystallize in three different structures at room temperature [19,20]. One belongs to I2/a symmetry or M-type (fergusonite structure), the other is P2/a symmetry or M´-type, which is true equilibrium phase at room temperature with the M-type modification and another is the high temperature tetragonal phase of the scheelite structure or T-type. As shown in Fig. 2, the NTO film coincides with tetragonal T-$NdTaO_4$ and monoclinic M´-$NdTaO_4$ phases. From XRD patterns it resulted that the tetragonal phase transforms to M phase in $NdNbO_4$ films or M´ phase in $NdTaO_4$ films.

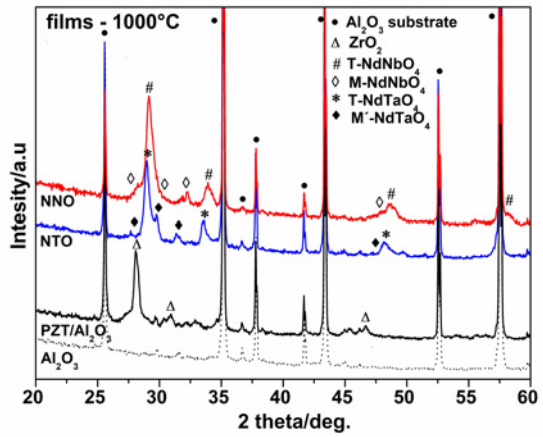

Fig.2 XRD patterns of $NdNbO_4$ and $NdTaO_4$ thin films on PZT/Al_2O_3 substrates after annealing at 1000°C.

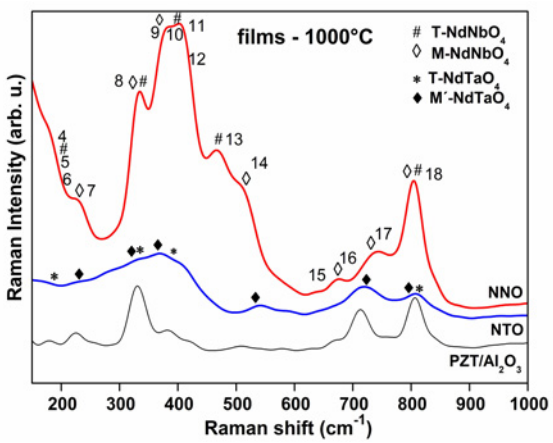

Fig.3. Raman spectra of $NdNbO_4$ and $NdTaO_4$ thin films on PZT/Al_2O_3 substrates after annealing at 1000°C.

Raman spectra of the films after annealing at 1000°C are shown in Fig. 3. The 18 optical Raman active phonon modes are expected [21,22]. Two dominant bands at 330 cm^{-1} and 800-805 cm^{-1} were clearly identified in all films. These bands are assigned as the bending and stretching modes of MO_6 ($M=Nb^{5+},Ta^{5+}$) octahedron, respectively. The intense three peaks at 331, 420 and 465 cm^{-1} or peak between 600 and 850 cm^{-1} are visible in NNO. Similar doublets assigned tetragonal T-$NdTaO_4$ and monoclinic M´-$NdTaO_4$ structure was found in the spectra of NTO thin film. Frequencies in range 230-450 cm^{-1} are influenced by Nd^{3+} cation displacements. 550-850 cm^{-1} range could be assigned to the Nb-O or Ta-O stretching modes essentially involving oxygen atom shifts [22]. Two new peaks in the around 537 and 730 cm^{-1} in $NdTaO_4$ film appeared and correspond to luminescence spectra. The phase composition and list of the observed frequencies of the Raman-active bands of NNO and NTO films were included in Table 1.

Tab.1. Phase composition and a list of the observed frequencies of the Raman-active bands of $NdNbO_4$ and $NdTaO_4$ films annealed at 1000°C.

Films	NNO	NTO
Phase composition	Tetragonal T-$NdNbO_4$ (81-1974) Monoclinic M-$NdNbO_4$ (32-0680)	Tetragonal T-$NdTaO_4$ (16-0745) Monoclinic M´-$NdTaO_4$ (83-0408)
Raman mode (Wavenumbers [cm^{-1}])	4 (180.1), 7 (229.4), 9 (331.0), 11 (377.2), 12 (407.2), 14 (471.2), 17 (674.5), 18 (803.1)	4 (174.2), 7 (210.2), 9 (323.4), 11 (372.4), 12 (403.2), 14 (490.3), 17 (678.2), 18 (810.1)

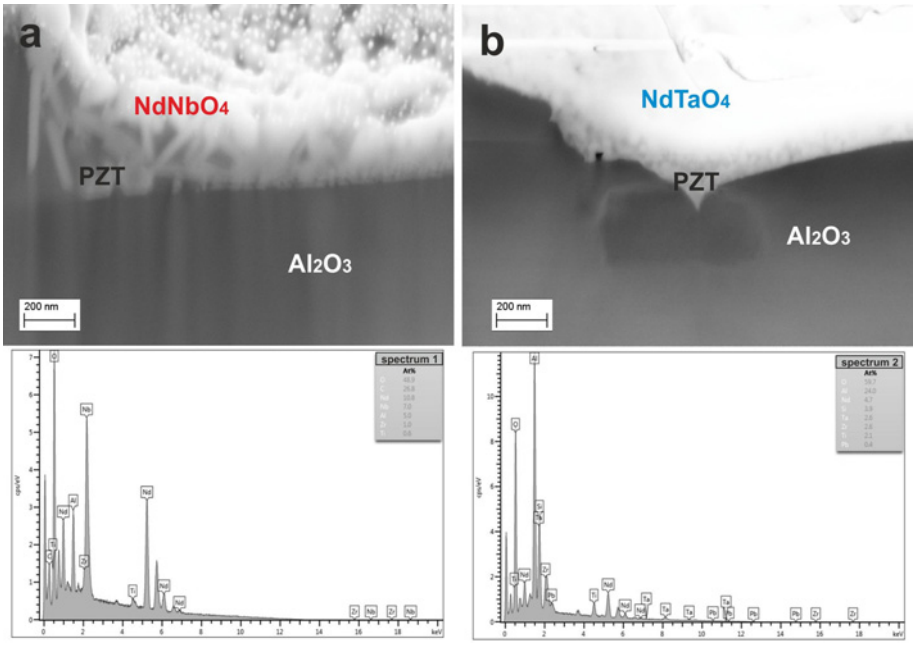

Fig. 4 FIB-SEM cross-section microstructures of (a) NNO/PZT/Al_2O_3, (b) NTO/PZT/Al_2O_3 thin films and EDS spectra 1 and 2.

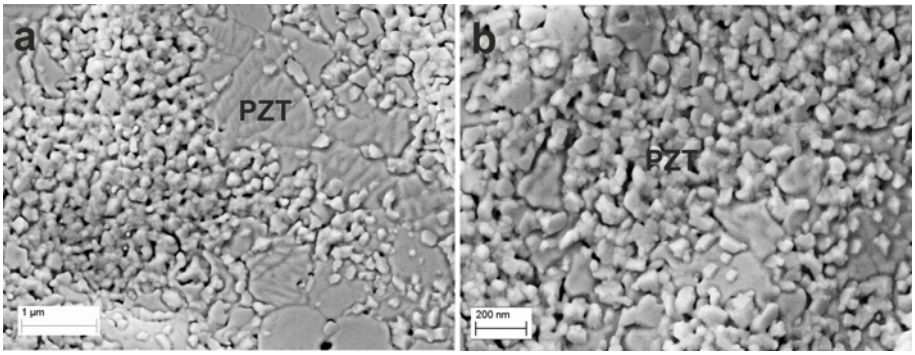

Fig. 5 SEM surface microstructures of PZT interlayer on Al_2O_3 substrate annealed at 1000°C with different resolution of (a) 1 μm and (b) 200 nm.

The cross-section microstructure of NNO (Fig.4) thin film deposited on PZT/Al_2O_3 substrate was characterized using SEM equipped with a focused ion beam (FIB-SEM). From image analysis of film it resulted that the NNO (Fig. 4a), NTO (Fig.4b) films and PZT layer thickness was ~100 and ~50 nm, respectively. EDS analyses demonstrate the distribution of elements across NNO (spektrum 1) and NTO (spektrum 2) films and results confirm the presence of Nd, Nb or Ta, in the films, Pb, Zr, Ti from PZT interlayer and Al, O from Al_2O_3 substrate.

Fig. 5a,b demonstrates the SEM micrographs of PZT interlayer on Al_2O_3 substrate. The film microstructures contained two phases (monoclinic ZrO_2 and pyrochore PZT). Pyrochlore $Pb_2(Zr, Ti)_2O_7$ phase [23] occurs at 29° (222), 33° (400) and 45°(200) and was not confirmed by XRD in Fig. 2 (one PZT layer - only 50 nm thickness).

The SEM micrographs of the NNO and NTO thin films are shown in Fig. 6. It was observed that the particles of the ceramic films were dense and uniform at the temperature 1000°C. The microstructure of NTO (Fig. 6b) film composed of $NdTaO_4$ was smoother than NNO film (Fig. 6a). The heterogeneous microstructure of the NTO is characterized by the bimodal particle size distribution and contains smaller spherical tetragonal $NdTaO_4$ (~ 30-50 nm) and bigger monoclinic $NdTaO_4$ particles of about ~100 nm. EDS analyses demonstrate the distribution of elements across NNO (spektrum 1) and NTO (spektrum 2) films and results confirm the presence of Nd, Nb or Ta, in the films. We described that 3 layers were deposited on substrate. We observed this preparation step in the final structures of perovskite interlayer $Pb(Zr_{0.52}Ti_{0.48})O_3/Al_2O_3$ and pyrochlore $NdNbO_4/Pb(Zr_{0.52}Ti_{0.48})O_3/Al_2O_3$ or $NdTaO_4/Pb(Zr_{0.52}Ti_{0.48})O_3/Al_2O_3$ films. The thickness of $Pb(Zr_{0.52}Ti_{0.48})O_3$ (PZT) and $NdNbO_4$ or $NdTaO_4$ thin films were ~ 50 and ~ 100 nm, respectively.

The 2D and 3D AFM micrographs of the PZT interlayer, NNO and NTO thin films are shown in Figs. 7 and 8. The monoclinic $NdNbO_4$ phase shows type ferroelasticity rubber-like behavior (pseudoelasticity) found in NNO film (Fig. 8) and domain structure was observed in NNO precursor [24,25]. As shown in Fig. 8, the AFM image illustrates that average particle size in NTO film (~ 50-100 nm). The root mean square (R_q) surface roughness values of the films were calculated as 6.95 nm for NNO, 5.24 nm for NTO and 24 nm for PZT layer on Al_2O_3 substrate. The structural properties of NNO and NTO films are depending on their phase composition.

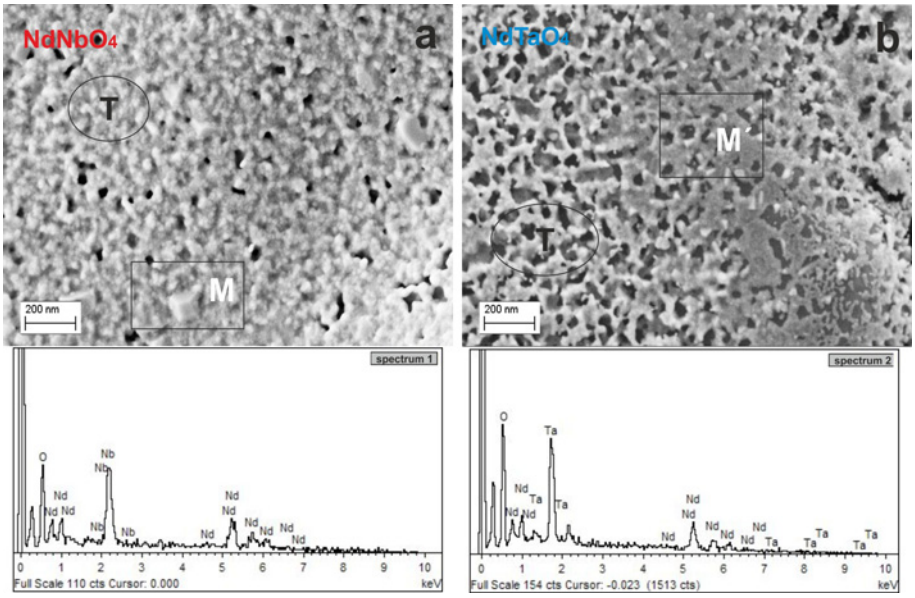

Fig. 6 SEM surface microstructures of $NdNbO_4$ (spektrum 1) and $NdTaO_4$ (spektrum 2) thin films annealed at 1000°C and EDS spectra.

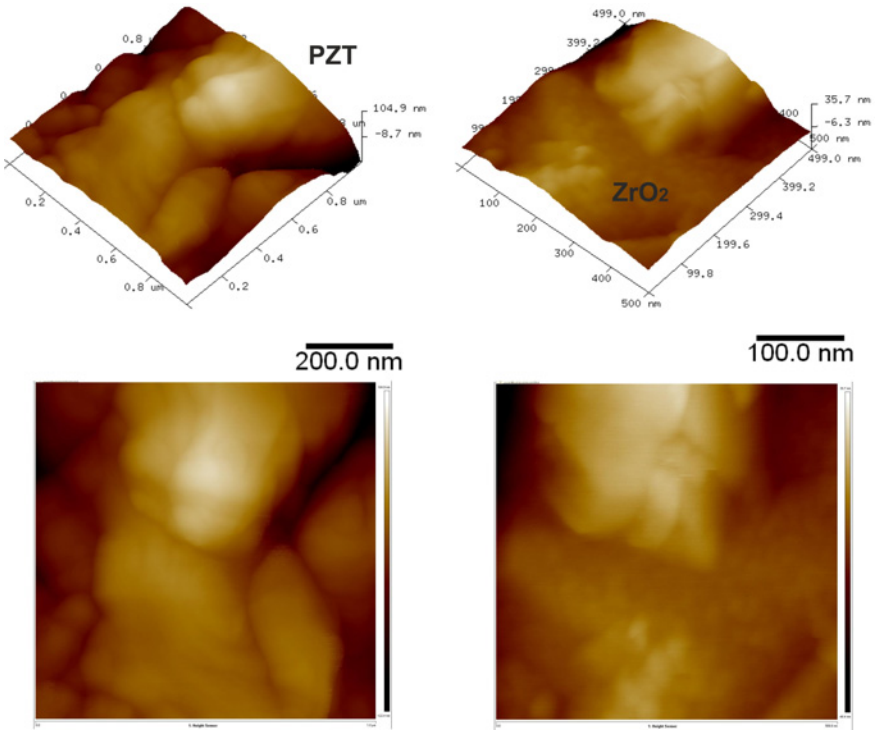

Fig.7. 2D and 3D AFM surface topography of PZT/Al_2O_3 substrate annealed at 1000°C.

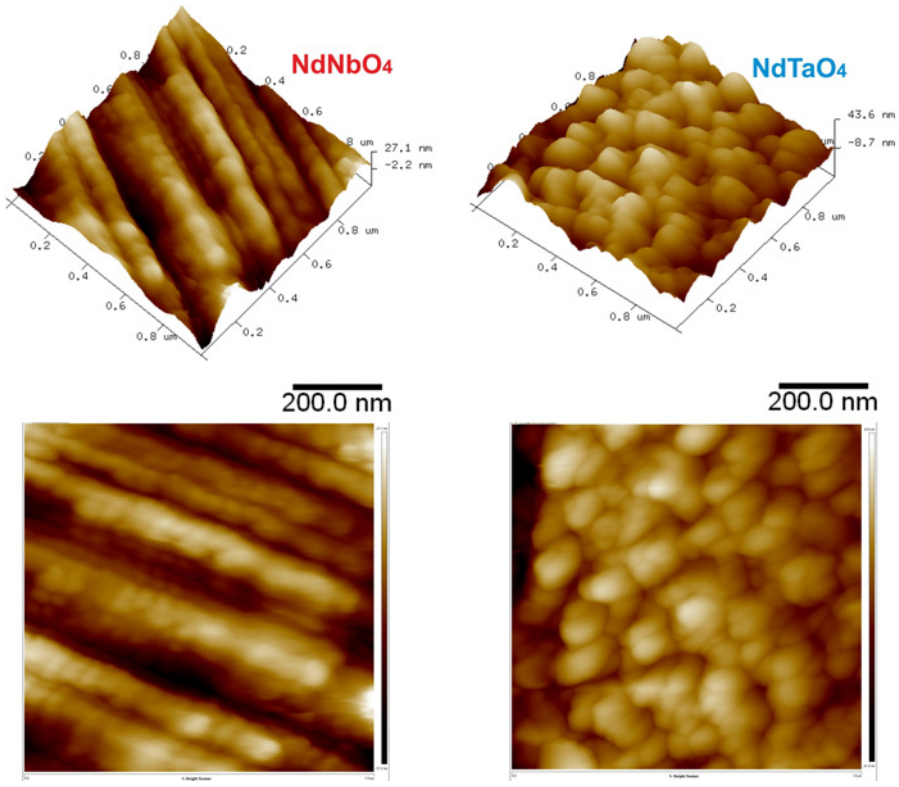

Fig.8. 2D and 3D AFM surface topography of $NdNbO_4$ and $NdTaO_4$ thin films annealed at 1000°C.

In the sol-gel process, the surface and properties of the films were crucially affected by the amount of carboxylic (citric or tartaric) acid [1]. The addition of tartaric acid could significantly increase the particle size and change the surface of NNO and NTO films. The shape and size of nanoparticles play an essential role in determining the electrolytic properties. The thermal evolution for NNO and NTO films showed that crystal phases are formed up to 1000ºC, while single well-crystallized M-$NdNbO_4$ or M´-$NdTaO_4$ materials are obtained in temperatures higher than 1000ºC. In future work, the influence of the annealing time will be investigated for the NNO and NTO films: a longer time is necessary to obtain thin films in the single monoclinic structure for application in environmental electrolytic thin film devices.

CONCLUSIONS

In conclusion, we have developed novel neodymium niobate and tantalate thin films using tartrate solutions. The ceramic $NdNbO_4$ (NNO) and $NdTaO_4$ (NTO) thin films (~100 nm) were prepared by sol-gel/spin-coating method on Al_2O_3 substrates with $Pb(Zr_{0.52}Ti_{0.48})O_3$ (PZT) interlayer and annealed at 1000°C.

The structural characterization of the films demonstrates strong different phase formation in NNO film in comparison with NTO. XRD results confirmed the major presence of tetragonal T-$NdNbO_4$ or T-$NdTaO_4$ and minor monoclinic M-$NdNbO_4$ or M´-$NdTaO_4$ phases in NNO and NTO thin films. The needle-like sharp features were identified

in the heterogeneous microstructure of $NdNbO_4$ film, which is different as compared with the Nd tantalate film composed of spherical particles (tetragonal $NdTaO_4$) and cuboidal (monoclinic $NdTaO_4$ phase).

It is found that the carboxylic acid has a strong morphological directing function. By using tartaric acid as the complexing agent, spherical and needle-like or cuboidal-shaped nanoparticles with different sizes and crystal phases could be obtained. The method reported here provides a new approach to preparing uniform NNO and NTO films. The results of this work can contribute to the fabrication of these films for application in environmental electrolytic thin film devices.

Acknowledgement

This work was supported by the Grant Agency of the Slovak Academy of Sciences through project No. 2/0036/17.

REFERENCES

[1] Mather, SA., Davies, PK.: J. Am. Ceram. Soc., vol. 78, 1995, p. 2737.
[2] Mei, QJ., Li, CY., Guo, JD., Zhao, LP., Wu, HT.: Ceram. Int., vol. 41, 2015, p. 907.
[3] Loiko, PA., Dymshits, OS., Alekseeva, IP., Zhilin, AA., Tsenter, MY., Vilejshikova, EV., Bogdanov, KV., Mateos, XK., Yumashev, KV.: J. Luminesc., vol. 179, 2016, p. 64.
[4] Siqueira, KPF., Carmo, AP., Bell, MJV., Dias, A.: J. Luminesc., vol. 138, 2013, p. 133.
[5] Ferrara, Ch., Mancini, A., Ritter, C., Malavasi, L., Tealdi, C.: J. Mater. Chem. A, vol. 3, 2015, p. 22258.
[6] Siqueira, KPF., Dias, A.: Mater. Res., vol. 17, 2014, p. 167.
[7] Titova, YA., Sych, AM., Sokolov, AN., Kapshuk, AA., Markiv, VY., Belyavina, NM.: J. Alloys Compd., vol. 311, 2000, p. 252.
[8] Zhang, P., Song, Z., Wang, Y., Han, Y., Dong, H., Li, L.: J. Alloys Compd., vol. 581, 2013, p. 741.
[9] Song, Z., Zhang, P., Wang, Y., Li, L.: J. Alloys Compd., vol. 583, 2014, p. 546.
[10] Hirano, M., Dozono, H.: Mater. Res. Bull., vol. 50, 2014, p. 213.
[11] Siqueira, KPF., Lima, PP., Ferreira, RAS., Carlos, LD., Bittar, EM., Matinaga, FM., Paniago, R., Moreira, RL., Dias, A.: J. Phys. Chem. C, vol. 119, 2015, p. 17825.
[12] Lu, Y., Tang, X., Yan, L., Li, K., Liu, X., Shang, M., Li, Ch., Lin, J.: J. Phys. Chem. C, vol. 117, 2013, p. 21792.
[13] Peng, H., Zhang, Y., Zhou, Y. C.: Prog. Nat. Sci.: Mater. Int., vol. 22, 2012, p. 219.
[14] Pontes, DSL., Pontes, FM., Pereira-da-Silva, MA., Zampieri, M., Chiquito, AJ., Pizani, PS., Longo, E.: Ceram. Int., vol. 40, 2014, p. 4085.
[15] Velu, G., Haccart, T., Jaber, B., Re`miens, D.: J. Vac. Sci. Technol. A: Vac. Surf. Films, vol. 16, 1998, p. 2442.
[16] Li, DH., Lee, ES., Chung, HW., Lee, SY.: Appl. Surf. Sci., vol. 252, 2006, p. 4541.
[17] Brunckova, H., Medvecky, L., Briancin, J., Durisin, J., Mudra, E., Sebek, M., Kovalcikova, A., Sopcak, T.: Mater. Lett., vol. 165, 2016, p. 239.
[18] Brunckova, H., Medvecky, L., Briancin, J., Saksl, K.: Ceram. Int., vol. 30, 2004, p. 453.
[19] Xiao, X., Yan, B.: J. Mater. Res., vol. 23, 2008, p. 679.
[20] Wang, J., Chong, X., Zhou, R., Feng, J.: Scripta Mater., vol. 126, 2017, p. 24.
[21] Siqueira, KPF., Dias, A.: Mater. Res., vol. 17, 2014, p. 167.
[22] Siqueira, KPF., Moreira, RL., Dias, A.: Chem. Mater., vol. 22, 2010, p. 2668.
[23] Yue, J., Leung, M., Haemmerle, E., Hodgson, M., Li, G., Gao, W.: J. Alloys Compd.,

vol. 470, 2009, p. 465.
[24] Tsunekawa, S., Takei, H.: Phys. Status Solidi A, vol. 50, 1978, p. 695.
[25] Kuroiwa, Y., Nozawa, K., Ikegami, J., Shobu, T., Noda, Y.: J. Korean Phys. Soc., vol. 32, 1998, p. 84.